Calculations of unsteady viscous flow past a circular cylinder

By R. B. PAYNE
Computing Machine Laboratory, University of Manchester

(*Received* 1 *November* 1957)

SUMMARY

A numerical solution has been obtained for the starting flow of a viscous fluid past a circular cylinder at Reynolds numbers 40 and 100. The method used is the step-by-step forward integration in time of Helmholtz's vorticity equation. The advantage of working with the vorticity is that calculations can be confined to the region of non-zero vorticity near the cylinder.

The general features of the flow, including the formation of the eddies attached to the rear of the cylinder, have been determined, and the drag has been calculated. At $R = 40$ the drag on the cylinder decreases with time to a value very near that for the steady flow.

1. INTRODUCTION

The general features of the flow of a viscous fluid past a circular cylinder are known from experiments. At low Reynolds numbers a steady symmetrical flow exists. At Reynolds numbers above about 40 the symmetrical flow is unstable and periodic oscillations known as the Kármán vortex sheet appear. Numerical solutions of the steady flow have been obtained at Reynolds numbers 10 and 20 by Thom (1933) and at $R = 40$ by Kawaguti (1953).

In this paper the two-dimensional flow of a viscous fluid started impulsively from rest and moving perpendicular to the axis of a circular cylinder is investigated. Apart from its intrinsic interest, this flow is expected to throw light on the high speed flow around yawed bodies of revolution. The method employed, which is the integration of Helmholtz's vorticity equation, is that which was used by the author (Payne 1956) for the starting and perturbation of a two-dimensional jet. The preliminary results, described below, were obtained for the starting flow past a circular cylinder at Reynolds numbers 40 and 100. In these calculations no asymmetry was introduced. With the aid of a more powerful electronic computer, it is intended to proceed to higher Reynolds numbers and also to investigate the unsymmetrical flow.

2. Equations of motion and boundary conditions

Use is made of Helmholtz's vorticity equation with allowance for viscosity,

$$\frac{\partial\omega}{\partial t}+\frac{\partial(u\omega)}{\partial x}+\frac{\partial(v\omega)}{\partial y}=\frac{2}{R}\left\{\frac{\partial^2\omega}{\partial x^2}+\frac{\partial^2\omega}{\partial y^2}\right\}, \tag{1}$$

R being the Reynolds number, to find the vorticity ω at successive small intervals of time. (The cylinder has unit radius and the velocity at infinity is unity.) The velocity (u, v) is found by adding to the velocity of the classical inviscid steady flow the velocity due to the vorticity, which is given by

$$\left.\begin{aligned} u(x,y,t) &= -\frac{1}{2\pi}\iint \omega(X,Y,t)\,\frac{(y-Y)}{(x-X)^2+(y-Y)^2}\,dXdY,\\ v(x,y,t) &= \frac{1}{2\pi}\iint \omega(X,Y,t)\,\frac{(x-X)}{(x-X)^2+(y-Y)^2}\,dXdY. \end{aligned}\right\} \tag{2}$$

The boundary condition that on the cylinder there is no flow perpendicular to the surface is satisfied by introducing image vorticity, while the no-slip condition causes vorticity to be generated on the cylinder. The vorticity is diffused and convected away, giving a region of non-zero vorticity near the cylinder. The calculations are confined to this region.

It is convenient to use coordinates $\zeta = \log r$, where r is the radial distance, and θ, the azimuthal angle. Helmholtz's vorticity equation becomes

$$r^2\frac{\partial\omega}{\partial t}+\frac{\partial}{\partial\xi}(rU\omega)+\frac{\partial}{\partial\theta}(rV\omega)=\frac{2}{R}\left\{\frac{\partial^2\omega}{\partial\xi^2}+\frac{\partial^2\omega}{\partial\theta^2}\right\}, \tag{3}$$

where U and V are the radial and transverse components of velocity.

3. Finite differences

The plane is covered by a mesh of points $\xi = k\Delta$, $\theta = j\Delta$, where k and j are integers and Δ is a constant. From equation (3), and replacing the space derivatives by central difference formulae and using a forward difference for the time derivative, a first approximation to the vorticity at the next step in time is

$$\Omega^{(n+1)}_{k,j} = \omega^{(n)}_{k,j}+\Delta t\,F(U^{(n)}_{K,J},\ V^{(n)}_{K,J},\ \omega^{(n)}_{K,J})$$

where

$$\begin{aligned} F(U^{(n)}_{K,J},\ V^{(n)}_{K,J},\ \omega^{(n)}_{K,J}) = \frac{1}{2r_k^2\Delta}\{&r_{k-1}\,U^{(n)}_{k-1,j}\,\omega^{(n)}_{k-1,j}-r_{k+1}\,U^{(n)}_{k+1,j}\,\omega^{(n)}_{k+1,j}\ +\\ &+r_k\,V^{(n)}_{k,j-1}\,\omega^{(n)}_{k,j-1}-r_k\,V_{k,j+1}\,\omega^{(n)}_{k,j+1}\}+\\ &+\frac{2}{Rr_k^2\Delta^2}\{\omega^{(n)}_{k+1,j}+\omega^{(n)}_{k-1,j}+\omega^{(n)}_{k,j+1}+\omega^{(n)}_{k,j-1}-4\omega^{(n)}_{k,j}\}. \end{aligned}$$

The velocity at time $(n+1)\Delta t$ is then evaluated from the integrals (2), as approximated by equations (6), below giving

$$U^{(n+1)}_{K,J} = U_{K,J}(\Omega^{(n+1)}_{p,q}), \qquad V^{(n+1)}_{K,J} = V_{K,J}(\Omega^{(n+1)}_{p,q}).$$

Then a second approximation to the vorticity at time $(n+1)\Delta t$ is

$$\omega_{k,j}^{(n+1)} = \tfrac{1}{2}\Omega_{k,j}^{(n+1)} + \tfrac{1}{2}\{\omega_{k,j}^{(n)} + \Delta t\, F(U_{K,J}^{(n+1)},\ V_{K,J}^{(n+1)},\ \Omega_{K,J}^{(n+1)})\}. \tag{4}$$

Since the vorticity at each lattice-point is Δ^{-2} times the circulation around a quadrilateral of area Δ^2 centred on the point, and this circulation is $V\Delta$ if the transverse velocity is V just away from the surface and 0 on the surface, the vorticity at points on the cylinder is given by

$$\omega_{0,j}^{(n+1)} = V_{0,j}^{(n+1)}/\Delta. \tag{5}$$

The velocity due to the vorticity is obtained from the formulae

$$\left.\begin{aligned} \frac{r_k\, U_{k,j}^{(n+1)}}{\Delta} &= \sum_{m=1}^{\infty}\sum_{l=1-\pi/\Delta}^{\pi/\Delta} (A_{k-m,j-l} - A_{k+m,j-l}) r_m^2\, \Omega_{m,l}^{(n+1)}, \\ \frac{r_k\, V_{k,j}^{(n+1)}}{\Delta} &= \sum_{m=1}^{\infty}\sum_{l=1-\pi/\Delta}^{\pi/\Delta} \left(B_{k-m,j-l} - B_{k+m,j-l} + \frac{\Delta}{2\pi}\right) r_m^2\, \Omega_{m,l}^{(n+1)}, \end{aligned}\right\} \tag{6}$$

where

$$A_{a,b} = -\frac{\Delta}{2\pi}\frac{\sin b\Delta}{\exp(a\Delta)+\exp(-a\Delta)-2\cos b\Delta} \qquad \text{if } a \neq 0 \text{ or } b \neq 0,$$

$$B_{a,b} = \frac{\Delta}{2\pi}\frac{\exp(a\Delta)-\cos b\Delta}{\exp\ (a\Delta)+\exp(-a\Delta)-2\cos b\Delta} \qquad \text{if } a \neq 0 \text{ or } b \neq 0,$$

and

$$A_{0,0} = B_{0,0} = 0.$$

4. Drag

The total drag on the cylinder is equal to the rate of decrease of momentum of the fluid, from which it follows (Phillips 1956) that

$$D = -\frac{d}{dt}\left\{\iint_{x^2+y^2\geqslant 1} py\omega\, dxdy\right\}.$$

The drag coefficient is $C_D = D/(\frac{1}{2}\rho U_\infty^2\, 2r_0)$ (where $r_0 = U_\infty = 1$ in our calculation, r_0 being the radius of the cylinder). Using the coordinates ξ and θ, and replacing the double integral by a double sum, the drag coefficient at time $(n+\frac{1}{2})\Delta t$ is found as

$$C_D = -\frac{1}{\Delta t}\left[\sum_{k=0}^{\infty}\sum_{l=1-\pi/\Delta}^{\pi/\Delta} r_k^3 \sin j\Delta\, \omega_{k,j}^{(n)}\, \Delta^2\right]_n^{n+1}$$

For Reynolds number 40 the drag coefficient thus calculated was initially 3·00, decreasing rapidly to 1·91 after unit time (the time in which the fluid at infinity moves a distance equal to the radius of the cylinder) and thereafter decreasing more slowly (see figure 1). At $t = 6$ it is about 2% above the value $C_D = 1{\cdot}6177$ calculated by Kawaguti for the steady flow at $R = 40$. For Reynolds number 100, the drag coefficient was initially 1·20, decreasing to a minimum of 1·00 just before $t = 1$ and rising to 1·10 at $t = 3$. It is easily shown that for all Reynolds numbers there is also an impulsive drag coefficient of π when the flow is started.

For small t, the boundary layer is very thin so the value of C_D given by equation (8) will not be accurate. The coarse mesh will not satisfactorily cover the flow within the boundary layer itself. In this range of t it is necessary to use the boundary layer solution of the equations of motion.

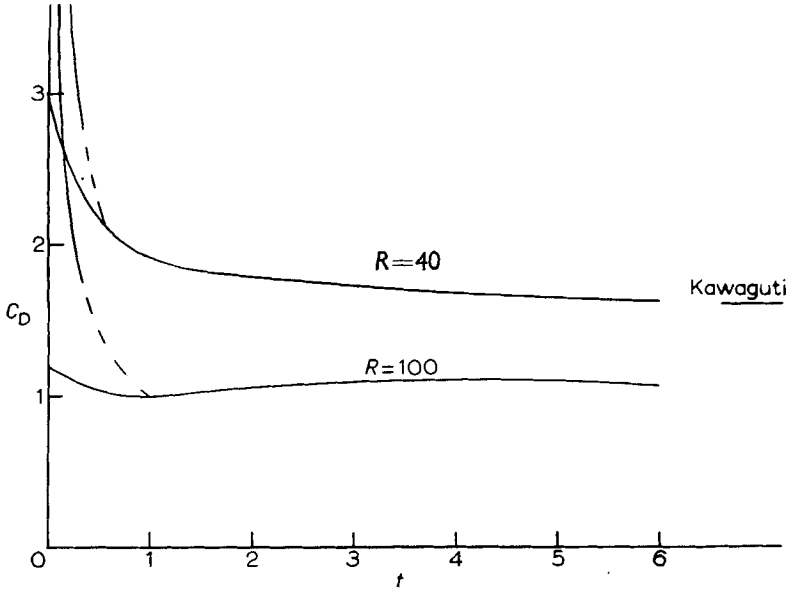

Figure 1. The variation of the drag coefficient with time for the starting flow past a circular cylinder. The value obtained by Kawaguti for the steady flow at Reynolds number 40 is also shown, together with the analytical solution for small t. The boundary layer solution is not valid beyond the instant at which separation occurs; however, beyond separation it is shown as a broken line suggesting a method of joining it to the numerical solution.

To the first approximation as $t \to 0$ (Goldstein & Rosenhead 1936),

$$V = -2\sin\theta \frac{2}{\sqrt{\pi}} \int_0^\eta \exp(-x^2)\, dx, \qquad \text{where } \eta = \frac{r-1}{2\sqrt{(\nu t)}}.$$

Hence

$$\omega = -\frac{2\sin\theta}{\sqrt{(\pi\nu t)}} \exp(-\eta^2).$$

From equation (7) it then follows that

$$\begin{aligned} C_D &= -\frac{d}{dt}\left\{ \int_{r=1}^{\infty} \int_{\theta=0}^{2\pi} \omega r^2 \sin\theta \, dr d\theta \right\} \\ &= \frac{d}{dt}\{2\pi + 8\sqrt{(\pi\nu t)} + O(t)\} \\ &\sim 4\sqrt{(2\pi/Rt)} \qquad \text{as} \quad t \to 0. \end{aligned}$$

This is also shown in figure 1. It is interesting to note that skin friction and pressure contribute equally to the total drag for small t, the respective drag coefficients being $2\sqrt{(2\pi/Rt)}$. Since the boundary layer ultimately separates, this value of the drag will not be reliable beyond (at most) $t = 0{\cdot}32$, when separation occurs (according to the boundary layer solution).

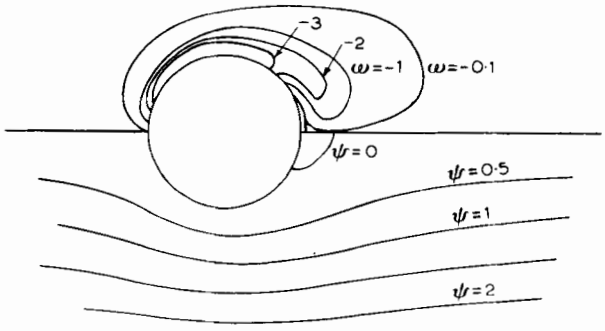

Figure 2. The symmetrical starting flow past a circular cylinder at Reynolds number 100 at time 2. In the upper half is shown the vorticity distribution and in the lower half the streamlines, the direction of flow being from left to right. The vorticity at the rear of the cylinder causes a reversed flow near the rear stangation point.

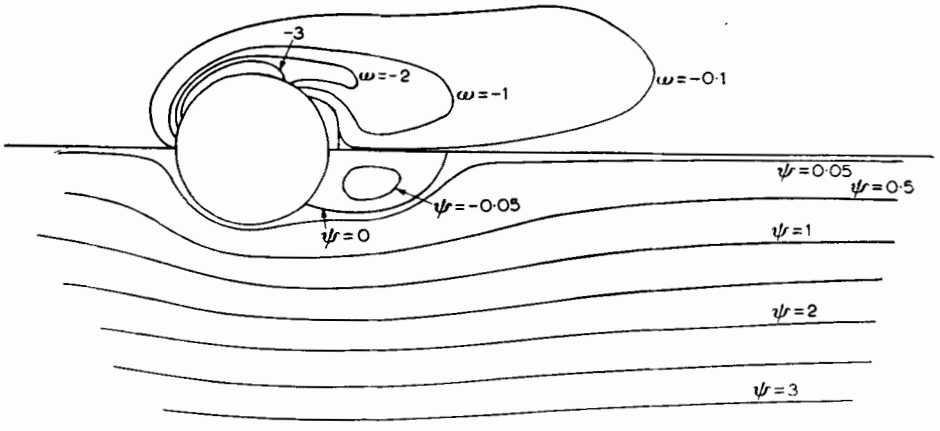

Figure 3. The symmetrical starting flow at Reynolds number 100 at time 6. The two eddies attached to the rear of the cylinder have increased in size.

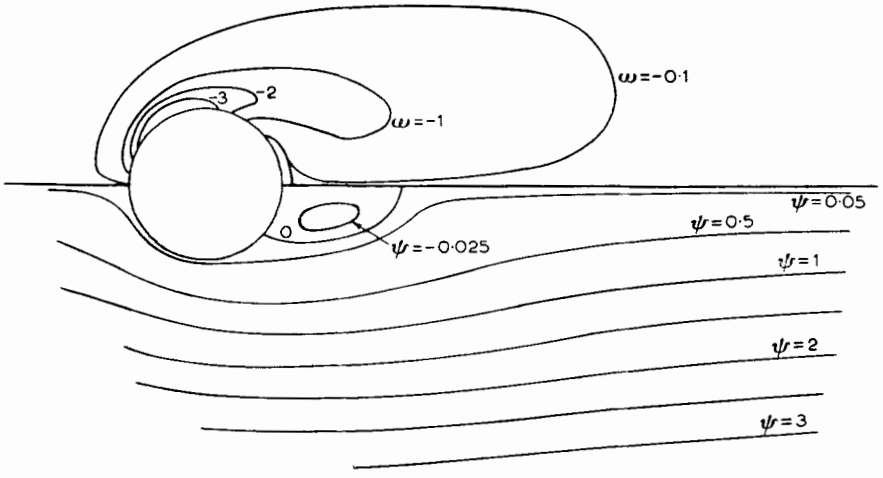

Figure 4. The symmetrical starting flow at Reynolds number 40 at time 6. The vorticity spreads further out laterally at this lower Reynolds number and there is a greater reduction in the velocity near the cylinder.

5. Results

The symmetrical flow past a cylinder starting impulsively from rest has been calculated for Reynolds numbers 100 (figures 2 and 3) and 40 (figure 4). The space mesh size used was $\Delta = \frac{1}{15}\pi = 0{\cdot}20944$ so that there were 30 mesh points round the cylinder at intervals of 12 degrees. The time interval was taken as $\Delta t = 0{\cdot}1$.

The vorticity generated at the cylinder is transported round towards the rear stagnation point. This vorticity induces a reversed flow on the cylinder, the velocity component at the mesh points nearest the rear stagnation point changing sign at $t = 1{\cdot}5$. The two eddies attached to the rear of the cylinder appear and increase in size. At $t = 6{\cdot}0$ they have spread 1·5 radii downstream (at both Reynolds numbers 100 and 40), which is about half the length of the standing eddies in Kawaguti's steady flow at Reynolds number 40.

At the two Reynolds numbers the starting flow is similar except that vorticity is spread over a larger area for $R = 40$ than for $R = 100$. The velocity within and near the rear eddies is also much smaller for the lower Reynolds number. For the drag coefficients in the two cases see figure 1.

References

Goldstein, S. & Rosenhead, L. 1936 *Proc. Camb. Phil. Soc.* **32,** 392.

Kawaguti, M. 1953 *J. Phys. Soc. Japan* **8,** 747.

Payne, R. B. 1956 *Aero. Res. Counc.* (*Lond.*), *Rep. & Mem.* no. 3047.

Phillips, O. M. 1956 *J. Fluid Mech.* **1,** 607.

Thom, A. 1933 *Proc. Roy. Soc.* A, **141,** 651.